Binding of the Inclusion Complex of Atorvastatin-β-cyclodextrin to Bovine Serum Albumin

N. Sudha[a], Y. Israel V.M.V. Enoch[b],* and Y. Sameena[c],*

[a]Department of Chemistry, Muthayammal College of Arts and Science, Rasipuram 637408, Tamil Nadu, India
[b]Department of Chemistry & Department of Nanoscience, Karunya Institute of Technology and Sciences (Deemed-to-be University),
Coimbatore 641114, Tamil Nadu, India
[c]Department of Chemistry, Sri Shakthi Institute of Engineering and Technology, Coimbatore 641062, Tamil Nadu, India

The objective of the paper is to determine the effect of β-cyclodextrin complexation on the interaction of the popular drug, Atorvastatin to bovine serum albumin. Fluorescence and 2D Rotating-frame Overhauser effect spectroscopic techniques are used to determine the stoichiometry, the binding contant, and the mode of binding of Atorvastatin to β-cyclodextrin. The role of the Atorvastatin-β-cyclodextrin complexation in modulating the binding strength of the drug to the model carrier protein bovine serum albumin is studied using absorption and fluorescence spectral measurements and molecular docking. Atorvastatin shows a fluorescence enhancement on comlplex formation with β-cyclodextrin. The results of the binding of the drug to bovine serum albumin in free- and β-cyclodextrin-bound forms. The magnitude of quenching of the fluorescence of bovine serum albumin due to drug binding, an d the Förster energy transfer efficiency between the protein and the drug are decreased in the presence of β-cyclodextrin. The binding constant value of the drug–protein binding in the absence and presence of β-cyclodextrin are 5.36×10^4 M^{-1} to 2.32×10^4 M^{-1}, respectively. Atorvastatin forms a 1:2 inclusion complex with cyclodextrin. The isopropyl substituent in the pyrrole ring of Atorvastatin binds to β-cyclodextrin. Cyclodextrin modulated the binding of drug to the serum albumin, *i.e.*, the cyclodextrin complex of Atorvastatin binds to bovine serum albumin with diminished binding strength. Nevertheless, the exposed part of the drug is found to be sufficient for interaction with the same binding pocket as the free drug binds to.

Keywords: β-cyclodextrin, Atorvastatin, Fluorescence, FRET, Bovine serum albumin, 2D ROESY

INTRODUCTION

Atorvastatin (ATR) is a member of the class of statins and has the trade name 'Lipitor'. It regulates lipoprotein metabolism [1,2] and decreases the incidence of cardiovascular disease in high-risk subjects, including those with the metabolic syndrome [3-5]. It inhibits hydroxymethylglutaryl (HMG) CoA, thereby decreasing

cholesterol biosynthesis, and reciprocally upregulating hepatic receptor-mediated clearance of apoB-containing lipoproteins [6,7]. It also controls acute coronary syndrome and thrombotic stroke [8,9], and regulates dyslipoproteinemia in the metabolic syndrome [10].

Bovine serum albumin, the most abundant protein in the circulatory system (a model protein), is a transport protein of small molecules [11,12]. It is circulated in the body several times and acts as carriers for numerous exogenous and endogenous compounds. It is capable of binding a diverse range of metabolites, drugs and organic

_____

*Corresponding authors. E-mail: drisraelenoch@gmail.com; sameen_y@yahoo.co.in

compounds. The remarkable binding properties of albumin account for the central role it can play in the efficacy and rate of delivery of drugs. Many drugs, including anti-coagulants, tranquilisers and general anesthetics, are transported in the blood, being bound to albumin [13]. BSA has an intrinsic structural homology of about 80% with human serum albumin [14,15]. It possesses a wide range of physiological functions associated with the binding, transport and distribution of biologically active compounds. The binding affinity of the drugs to serum albumins also influences the effectiveness of the drugs at the active site. Thus, the study of the interactions of small drug molecules to serum albumins provides a good insight into an understanding of the recognition pattern under physiological conditions [16]. These studies may provide information of the structural features that determine the therapeutic effectiveness of drugs, and become an important research field in life sciences, chemistry and clinical medicine. The molecular interactions are often monitored *in vitro* by using spectroscopic techniques.

Cyclodextrins are truncated cone–shaped cyclic oligosaccharides consisting mainly of six (α-CD), seven (β-CD), and eight (γ-CD) D(+)-glucopyranose units [17,18]. They form inclusion complexes with various organic compounds of suitable polarity and dimension, and improve the chemical reactivity, solubility, stability, and bioavailability of guest molecules. Cyclodextrins have two hydrophilic rims, where the hydroxyl groups are located, and a hydrophobic cavity capable of accommodating guest molecules [19-21]. The encapsulation of the drug molecule by cyclodextrin modifies the physical, chemical, and biochemical characteristics of the guest molecules [22,23]. Even though cyclodextrin-bound drugs are available and plenty of cyclodextrin complexes have been studied, reports on the binding of cyclodextrin-complexed drugs binding with serum albumins are quite scarce in the literature [24]. Inclusion complexation by β-CD is a phenomenon that plays a role in the delivery and sustained release of drugs which influences the pharmacokinetics of drugs. The present work deals with the interaction of ATR with BSA in the presence and absence of β-CD. We report that the encapsulation of ATR by β-CD modulates its binding to BSA.

EXPERIMENTAL

Materials

Atorvastatin hemicalcium trihydrate was purchased from Sigma-Aldrich, Bangalore, India. Crystalline bovine serum albumin, β-cyclodextrin, and HEPES (4-(2-hydroxy-ethyl)-1-piperazineethanesulfonic acid) were purchased from Hi Media, India. All the solvents, obtained from Merck, were of spectral grade, which were used as received.

Methods

Preparation of test solutions. Test solutions were prepared by an appropriate dilution of a stock solution of ATR (2.64×10^{-4} mol dm^{-3}). The stock solution of ATR was made in methanol due to its less solubility in water. Working solutions were prepared by an appropriate dilution of the stock solutions of ATR, β-CD, and BSA. The test solutions were having the concentration of ethanol as 1 %. HEPES buffer (0.1 M) was used to prepare the stock solution of BSA. All reagents and solvents used were of spectral grade which were used without further purification. Doubly distilled water was used throughout the experiments. All the experiments were carried out at an ambient temperature of 25 ± 2 °C. The test solutions were homogeneous after the addition of all the additives. The absorption and the fluorescence spectra were recorded against appropriate blank solutions.

Preparation of ATR/β-CD inclusion complex. ATR (0.223 g) was dissolved in 5 ml of methanol. 5 ml of aqueous β-CD (0.454 g) was prepared separately. A solution of ATR was added slowly to the β-CD solution at room temperature, sonicated using an ultra-sonicator, and maintained for 30 min to get a homogenous solution. The mixture was warmed to 50 °C for 10 min and kept at room temperature for two days. The solid obtained was collected and analyzed.

Instrumentation

A Jasco V-630, double beam UV-Vis spectrophotometer was used to record the absorption spectra. 1 cm path length cells were used for the measurements. A Jasco FP-750 spectrofluorimeter, equipped with a 120 W Xenon lamp for excitation, served

the measurement of fluorescence. Both the excitation and the emission band widths were set up at 5 nm. An ultra-sonicator (PCI 9L 250H, India) was used for sonication. The 2D ROESY spectra were recorded on a Bruker AV III instrument, operating at 500 MHz, with DMSO-d_6 as the solvent for the ATR-β-CD complex and the internal standard used was Tetramethylsilane (TMS). The chemical shift values were obtained downfield from TMS, in part per million (ppm). The 2D ROESY experiments were done on the prepared solid complexes of ATR-β-CD. The mixing time for ROSEY spectra was 200 ms under the spin lock condition.

RESULTS AND DISCUSSION

Host-guest Complex of β-CD with ATR

The host-guest association of ATR with β-CD was studied by UV-Vis absorption and fluorescence spectroscopy. The absorption spectra of ATR in water and in aqueous β-CD of different concentrations are shown in Fig. 1a. The absorption and fluorescence spectral data of the binding titration of ATR against β-CD are given in the Supporting Information (Table SI 1). In aqueous solution, ATR shows an absorption maximum at 240 nm (corresponding to the n-π* transition) and, with the addition of β-CD in aliquots, shows a hyperchromic shift. The absorption at 240 nm shows a large red shift of 273 nm with an increase in the concentration of β-CD (4.0×10^{-3} mol dm^{-3}). This may be due to complexation of ATR in β-CD and due to the surfactant action of β-CD.

The fluorescence spectra of ATR with various added amounts of β-CD are shown in Fig. 1b. With the addition of β-CD, ATR shows an enhancement of fluorescence along with a significant blue shift of about 3 nm. The observed increase of fluorescence intensity may be due to the restriction offered by the cavity of β-CD to the relaxation of ATR from the excited state and the non-polar environment the ATR molecule experiences on shifting from the polar environment in water to the apolar cavity of β-CD. The changes in the absorption and fluorescence spectra with the addition of β-CD suggest that there is a formation of host-guest complex of ATR with β-CD, which is represented by Eq. (1)

$$ATR + β\text{-}CD \rightleftharpoons ATR\text{-}β\text{-}CD \qquad (1)$$

The stoichiometry and the binding constant of the complex of ATR with β-CD were determined using the Benesi-Hildebrand equation [25]:

$$\frac{1}{I - I_0} = \frac{1}{I' - I_0} + \frac{1}{I' - I_0}\frac{1}{K[\beta - CD)} \qquad (2)$$

where I is the intensity at each concentration of β-CD, I_0 is the intensity of fluorescence of ATR in water and I′ is the intensity of fluorescence at the highest concentration of β-CD. K is the binding constant and it is calculated, in this case, as 3.21×10^5 M^{-2}. The linearity observed of the plot $1/(I' - I_0)$ *vs.* $1/[β\text{-}CD]^2$ implies that the inclusion complex formed is having a stoichiometry of 1:2 [ATR:β-CD]. The plot is given in Fig. 1c.

In order to further confirm the 1:2 complex and to optimize the structure of the inclusion complex, a 2D ROESY spectrum was recorded (Fig. 2). Off-diagonal cross peaks observed between the dimethyl protons at the positions of 35 and 36, as well as the aromatic protons of ATR at positions 9 and 13, with the H3 proton of β-CD. Further the H11 proton in the N-phenyl ring of ATR interacted with H5 proton of β-CD, due to the engulfing of the phenyl ring by the hydrophobic cavity of β-CD. This occurs readily due to the free availability of phenyl ring. It follows that the dimethyl group attached to the pyrrole ring and N-phenyl ring of the carboxamide moiety in the ATR are encapsulated with the involvement of two β-CD molecules. The schematic picture of the inclusion of the ATR in β-CD is shown in Fig. 3.

Binding of ATR to BSA

The absorption spectra of BSA showed a hyperchromic shift continuously at each addition of ATR in increasing concentration, as shown in Fig 4a. The concentration of BSA (1×10^{-5} mol dm^{-3}) was fixed and ATR was added in increasing amounts. The absorption maximum of 278 nm, corresponding to the n → π* transition of tryptophan residues in BSA, got shifted to the shorter wavelength by 3 nm on the addition ATR. This might be due to the binding of ATR to BSA.
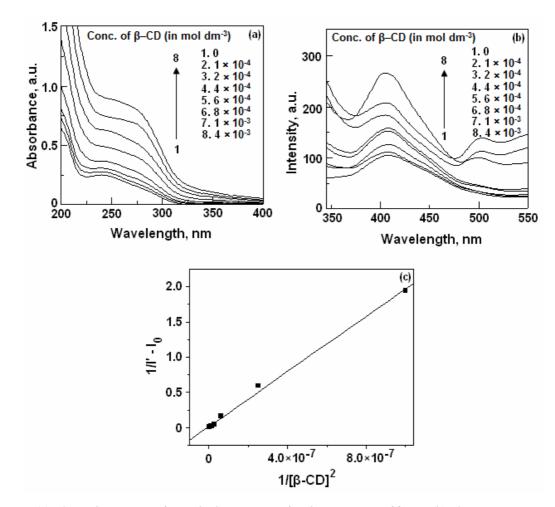
Fig. 1. (a) Absorption spectra of ATR in the presence of various amounts of β-CD. (b) Fluorescence spectra of ATR at various concentrations of β-CD. (c) Benesi-Hildebrand plot of the binding of ATR to β-CD.

The fluorescence quenching of BSA by ATR is shown in Fig. 4b. The change in the fluorescence spectrum was more pronounced than in absorption spectrum, when ATR was added to the BSA. The BSA molecule has an intrinsic fluorophore, tryptophan, which mainly contributes to its fluorescence. Addition of small molecules, usually causes a quenching of tryptophan fluorescence. When the excitation was done at 280 nm, BSA showed a strong fluorescence band at 347 nm, in aqueous solution. The fluorescence of BSA quenched continually with a blue shift of 9 nm at the successive additions of ATR in aliquots. The absorption and the fluorescence spectral data are compiled in Table SI 2 in the Supporting Information.
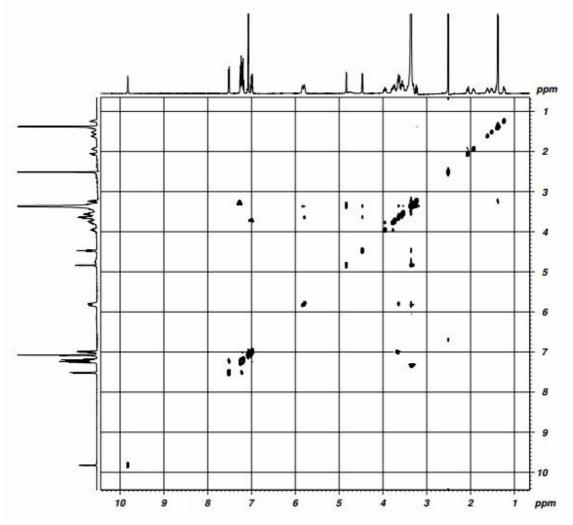
The correction of fluorescence intensity was determined by recording the absorbances at the wavelength of excitation and emission for each concentration of ATR and then multiplying the observed value of fluorescence intensity. The following relationship [26] was employed:

$$F_{corr} = F_{obs} \times e^{\frac{(A_{exi} + A_{emi})}{2}} \tag{3}$$

where, F_{corr} and F_{obs} refer to the the corrected and observed intensities of fluorescence, respectively, and A_{exi} and A_{emi} represent the absorbances at the excitation and emission wavelengths, respectively.

The fluorescence quenching may occur due to a variety of processes such as molecular rearrangements, excited state
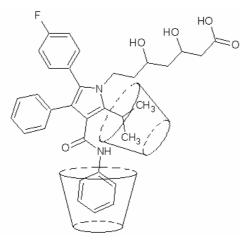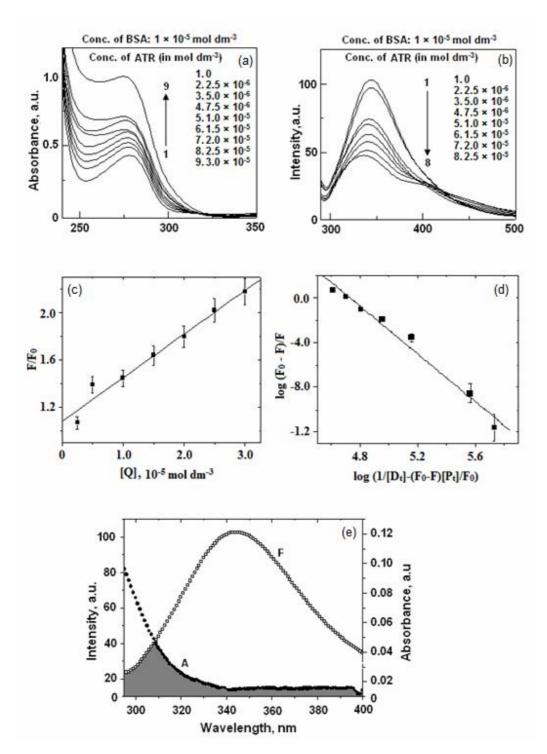
Fig. 2. 2D ROESY spectrum of the ATR-β-CD complex.

Fig. 3. Schematic diagram of the inclusion complex of ATR-β-CD.

Fig. 4. (a) Absorption spectra of BSA at various concentrations of ATR. (b) Fluorescence spectra of BSA at various concentrations of ATR. (c) Stern-Volmer ATR-BSA interaction. (d) The plot of $\log[F_0 - F]/F$ against $\log(1/[Dt] - (F_0 - F)/[Pt][F_0]$ of the interaction of BSA with various concentrations of ATR. (e) Spectral overlap between the absorption spectrum of ATR and the fluorescence spectrum of BSA.

reactions, energy transfer, ground state complex formation and collision processes. A collisional quenching between ATR and BSA was considered and analyzed by the popular Stern-Volmer equation [27]:

$$\frac{F_0}{F} = 1 + K_q \tau_0 [Q] = 1 + K_{SV}[Q] \qquad (4)$$

where F_0 and F are the fluorescence intensities of BSA in the absence and presence of the quencher (ATR) respectively. K_q is the biomolecular quenching rate constant and τ_0 is the lifetime of the BSA in the absence of quencher and $[Q]$ is the concentration of the quencher. The Stern-Volmer quenching constant is given by $K_{SV} = k_q\tau_0$. The Stern-Volmer plot (F_0/F *vs.* $[Q]$), of the quenching of fluorescence of BSA by ATR, is shown in Fig. 4c. The linearity of the Stern-Volmer plot is indicative of the fluorophores being equally accessible to the quencher. The value of K_{SV}, calculated from the plot, was 3.68×10^4 M^{-1}

The binding constant K_A and the number of binding sites were calculated from the Eq. (5),

$$\log \frac{F_0 - F}{F} = n\log K_A - n\log\left(\frac{1}{[D_t] - \frac{(F_0 - F)[P_t]}{F_0}}\right) \qquad (5)$$

Here, F_0 represents the initial intensity of fluorescence before the addition of the quencher and F denotes the fluorescence intensity of BSA at each addition of ATR. $[D_t]$ and $[P_t]$ refer to the concentration of the drug (ATR), and the total concentration of protein (BSA) respectively. The binding plot of $\log(1/[Dt] - (F_0-F)/[Pt][F_0]$ *vs.* $(F_0 - F)/F$ is shown in Fig. 4d. The calculated binding constant was 5.36×10^4 M^{-1} and the number of binding site was 0.9 (approximately 1). The value of the binding constant suggested that the binding between ATR and BSA was strong.

The distance between the tryptophan residue (donor) in BSA and the drug (acceptor) can be calculated according to Förster's resonance energy transfer theory (FRET) [28]. The overlap between the absorption spectrum of ATR with the fluorescence spectrum of BSA is shown in Fig. 4e, both the drug and the protein being within 8 nm distance of separation (R). The FRET efficiency (E) is given by the equation:

$$E = 1 - F/F_0 = R_0^6/R_0^6 + r_0^6 \qquad (6)$$

In this equation, r_0 is the distance between the ligand and the tryptophan residue of the protein, R_0 is the Förster distance at which the excitation energy transfer from donor (BSA) to the acceptor (ATR) is 50%. R_0 is calculated from the emission spectrum of the donor and the absorption spectrum of the acceptor, using the equation:

$$R_0^6 = 8.79 \times 10^{-25} \, K^2 \, N^{-4} \, \Phi \, J \qquad (7)$$
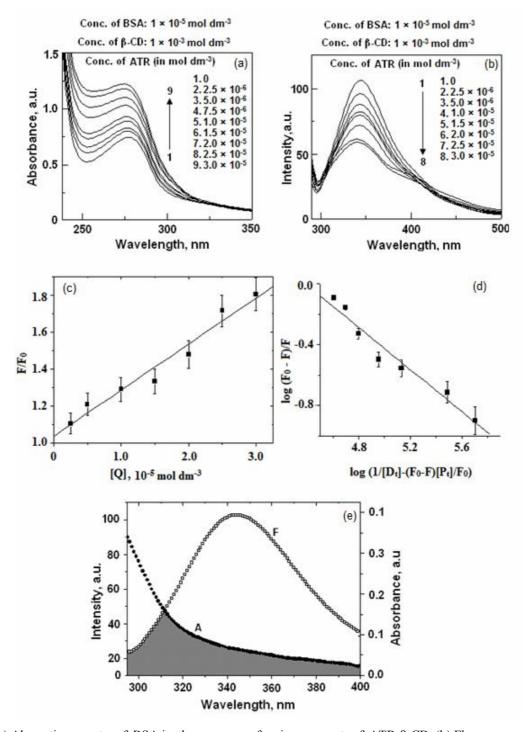
where K^2 is the relative orientation of the donor and the acceptor, N is the refractive index of the medium, Φ is the fluorescence quantum yield of the donor, and J is the overlap integral of the fluorescence spectrum of the donor and the absorption spectrum of the acceptor. The overlap integral, J is given by the equation:

$$J = \frac{\int_0^\infty F_D(\lambda)\varepsilon_A(\lambda_0)\lambda^4 d\lambda}{\int_0^\infty F_D(\lambda)d\lambda} \qquad (8)$$

where $F_D(\lambda)$ is the corrected fluorescence intensity of the donor in the wavelength range of λ and $(\lambda + \Delta\lambda)$, and $\varepsilon(\lambda)$ is the molar extinction coefficient of the acceptor at λ. We assumed random orientations of the donor and the acceptor. The donor to acceptor distance was 5.563 nm and R_0 was 3.825 nm. The value of N was 1.336, that of $K^2 = 2/3$, $\Phi = 0.15$, J $= 7.3896 \times 10^{-21}$ M^{-1} cm^{-1} nm^4 and E $= 0.0955$. The results confirmed that there occurred an energy transfer from BSA to ATR.

Binding of β-CD-encapsulated ATR with BSA

The ATR molecule is capable of binding to β-CD with a significant binding strength as discussed in the previous section. In order to understand the influence of β-CD in the interaction of ATR with BSA, a binding titration of the ATR-β-CD complex against BSA was carried out. Figure 5 (a) shows the absorption spectra of BSA with different concentrations of the ATR-β-CD complex. The absorption maximum shifted slightly towards the blue, at the addition of the ATR-β-CD. This indicates the binding of the ATR-β-

Fig. 5. (a) Absorption spectra of BSA in the presence of various amounts of ATR-β-CD. (b) Fluorescence spectra of BSA in the presence of various amounts of ATR-β-CD. (c) Stern-Volmer plot of the interaction of ATR-β-CD with BSA. (d) The plot of log$[F_0 - F]/F$ against log$(1/[Dt] - (F_0 - F)/[Pt][F_0]$ for the interaction of BSA with ATR-β-CD. (e) Spectral overlap between the absorption spectrum of ATR-β-CD and the fluorescence spectrum of BSA.
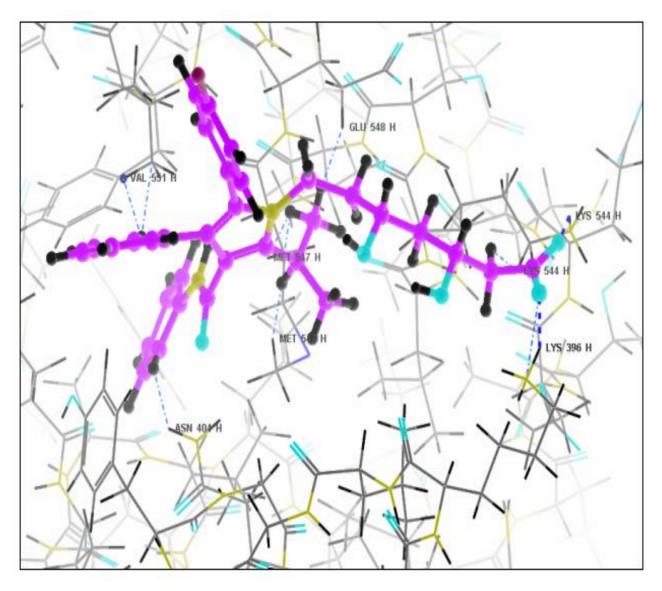
Fig. 6. Docking poses of ATR-BSA binding.

CD with BSA. The absorption and fluorescence spectral data of the binding of the ATR-β-CD are compiled in Table SI 3 (Supporting Information). The fluorescence spectra were measured with the excitation wavelength fixed at 280 nm. The observed quenching of fluorescence of BSA (with a blue shift of 3 nm) at the increase in the concentration of ATR-β-CD complex is shown in Fig, 5b. The Stern-Volmer plot for the quenching of fluorescence by the ATR-β-CD complex is shown in Fig. 5c. The plot of $\log(1/[Dt] - (F_0-F)[Pt]/F_0)$ *vs*. $\log(F_0 - F)/F$, of the binding of

the ATR-β-CD complex to BSA, is shown in Fig. 5d. The binding constant was determined as $2.32 \times 10^4\,M^{-1}$ and the number of binding sites was 0.67. The calculated binding constant is quite smaller than that observed for the quenching of free ATR-BSA in the absence of β-CD (*i.e.*, in water). Hence, encapsulation of ATR by β-CD decreased the direct collision of the ATR to the tryptophans in the binding pockets of the BSA.

Figure 5e shows the distance between the ATR-β-CD complex and the tryptophan residues of BSA calculated

from the FRET, as discussed earlier. The results were as follows: $J = 1.1127 \times 10^{-19}$ M^{-1} cm^{-1} nm^4, $R_0 = 2.434$ nm, $r = 3.795$ nm and $E = 0.0651$. The distance between donor and acceptor was less than that observed in the case of free ATR binding with BSA. Hence, β-CD clearly influenced the binding of ATR to BSA.

Molecular Docking

A further insight into the mode of the ATR–BSA binding was offered by molecular docking as shown in Fig. 6. BSA consists of three homologous domains (I, II and III): I (residues 1-183), II (184-376), III (377-583), each containing two sub-domains (A and B) that assemble to make it a heart shaped molecule. The best energy ranked results revealed that ATR was located within the sub-domain III hydrophobic cavity in close proximity to the residues, such as Glu-548, Val-551, Asn-404 and Met-547 suggesting the existence of hydrophobic interaction between them. Also, the acid group of 3,5-dihydroxy-7-(1H-pyrrol-1-yl)heptanoic acid moiety of ATR was involved in hydrogen bonding with Lys-544 and Lys-396 at a bond length of 2.051 Å and 1.733 Å, respectively. This hydrogen bonding increased the stability of the ATR-BSA bound system. As discussed in the previous section, we concluded that the dimethyl group attached to the pyrrole and N-phenyl ring of the carboxamide moiety of the ATR was engulfed by β-CD. Hence, the remaining part of the molecule standing outside the β-CD cavity bound to BSA. The binding constant value was, however, smaller than that in the case of free ATR binding to BSA. Hence, β-CD should have tended to extract ATR from BSA, due to its binding strength.

CONCLUSIONS

In summary, β-Cyclodextrin forms a 1:2 inclusion complex with ATR with a binding constant of 3.21×10^5 M^{-1}. The structure of the inclusion complex is proposed using fluorescence and NMR spectroscopic results. Interaction of ATR with BSA is carried out in water and in aqueous β-CD. Fluorescence quenching occurs and the calculated K_{SV} value is 3.68×10^4 M^{-1} for the ATR-BSA complex and the number of binding site is ≈ 1. Further, molecular docking confirm the interaction between the ATR

and BSA. FRET studies show that an energy transfer occurs between BSA and ATR. The K_{SV} (2.49×10^4 M^{-1}), the energy transfer efficiency and the number of binding sites are decreased when β-CD-complexed ATR binds to BSA. The dimethyl group, attached to the pyrrole and the N-phenyl ring of the carboxamide moiety of the ATR molecule, was encapsulated by the β-CD molecule and the remaining part of the molecule, standing outside the β-CD cavity, binds to BSA through hydrogen bonding and phobic interactions.

ACKNOWLEDGMENTS

CONFLICT OF INTEREST

No potential conflict of interest was reported by the authors.

REFERENCES

[1] F. Naeem, G. Mckay, M. Fisher, Br. J. Diabetes 18 (2018) 7.

[2] G.F. Watts, P.H.R. Barrett, J. Ji, A.P. Serone, D.C. Chan, K.D. Kroft, F. Loehrer, A.G. Johnson, Diabetes 52 (2003) 803.

[3] K. Ozaki, T. Kubo, R. Imaki, H. Shinagawa, H. Fukaya, K. Ohtaki, S. Ozaki, T. Izumi, Y. Aizawa, J. Atheroscler. Thromb. 13 (2006) 216.

[4] H. Pons-Rejraji, F. Brugnon, B. Sion, S. Maqdasy, G. Gouby, B. Pereira, G. Marceau, A.-S. Gremeau, J. Drevet, G. Grizard, L. Janny, I. Tauveron, Reprod. Biol. Endocrinol. 12 (2014) 65.

[5] A.F. Alghamdi, Curr. Anal. Chem. 14 (2018) 92.

[6] R.G. Bakker-Arkema, M.H. Davidson, R.J. Goldstein, J. Davignon, J.L. Isaacsohn, S.R. Weiss, L.M. Keilson, W.V. Brown, V.T. Miller, L.J. Shurzinske, D.M. Black, J. Am. Med. Assoc. 275 (1996) 128.

[7] W. Wang, W. Song, Y. Wang, L. Chen, X. Yan, J. Cardiovasc. Pharmacol. 62 (2013) 90.

[8] G.M. Rosa, F. Carbone, A. Parodi, E.A. Massimelli, C. Brunelli, F. Mach, N. Vuillieumer, F. Montecucco,

Eur. J. Clin. Investig. 44 (2014) 501.

[9]   K.L. Furie, Stroke 43 (2012) 1994.

[10] G. Zhou, S. Ge, D. Liu, G. Xu, R. Zhang, Q. Yin, W. Zhu, J. Chen, X. Liu, Cardiology 115 (2010) 221.

[11] A. Precupas, A.R. Leonties, A. Neacsu, R. Sandu, V.T. Popa, New J. Chem. 43 (2019) 3891.

[12] K.C. Ajithkumar, K. Pramod, Int. J. Appl. Pharm. 9 (2017) 95.

[13] W. Lian, Y. Liu, H. Yang, H. Ma, R. Su, X. Han, B. Zhao, L. Niu, Spectrochim Acta A 207 (2019) 307.

[14] M. Suganthi, K.P. Elango, Phys. Chem. Liq. 55 (2017) 165.

[15] A.K. Bordbar, N. Sohrabi, S. Tangestaninejad, Phys. Chem. Liq. 42 (2004) 127.

[16] A. Roy, D. Tripathy, A. Chatterjee, S. Dasgupta, J. Biophys. Chem. 1 (2010) 141.

[17] I.V.M.V. Enoch, M. Swaminathan, Coll. Czech. Chem. Commun. 69 (2004) 748.

[18] N. Sudha, I.V.M.V. Enoch, Phys. Chem. Liq. 57 (2019) 43.

[19] N. Sudha, Y. Sameena, S. Chandrasekaran, I.V.M.V. Enoch, D. Premnath, Spectrosc. Lett. 48 (2015) 112.

[20] N. Sudha, S. Chandrasekaran, D. Premnath, I.V.M.V. Enoch, Bull. Korean Chem. Soc. 35 (2014) 2114.

[21] I.V.M.V. Enoch, M. Swaminathan, J. Incl. Phenom. Macro. Chem. 53 (2005) 149.

[22] M. Murugan, A. Anitha, K. Sivakumar, R. Rajamohan, J. Solution Chem. 47 (2018) 906.

[23] A. Praveena, S. Prabu, R. Rajamohan, J. Macromol. Sci. A. 54 (2017) 894.

[24] N. Sudha, I.M.V. Enoch, J. Solution Chem. 40 (2011) 1755.

[25] H.A. Benesi, J.H. Hildebrand, J. Am. Chem. Soc. 71 (1949) 2703.

[26] J.R. Lakowicz, Principles of Fluorescence Spectroscopy, Springer: New York, 2009.

[27] Permyakov, A. Eugene, Luminescent Spectroscopy of Proteins. CRC Press, 1993.

[28] B. Valeur, M. Berberan-Santos, Molecular Fluorescence: Principles and Applications, 2nd ed. Weinheim: Wiley-VCH, 2012, pp. 213-261.